0026-895X/04/6606-1702–1711$20.00
MOLECULAR PHARMACOLOGY
Copyright © 2004 The American Society for Pharmacology and Experimental Therapeutics
Mol Pharmacol 66:1702–1711, 2004

Vol. 66, No. 6
4515/1185492
Printed in U.S.A.

Tibolone Is Metabolized by the 3α/3β-Hydroxysteroid Dehydrogenase Activities of the Four Human Isozymes of the Aldo-Keto Reductase 1C Subfamily: Inversion of Stereospecificity with a $\Delta^{5(10)}$-3-Ketosteroid

Stephan Steckelbroeck, Yi Jin, Busola Oyesanmi, Helenius J. Kloosterboer, and Trevor M. Penning

Department of Pharmacology, University of Pennsylvania School of Medicine, Philadelphia, Pennsylvania (S.S., Y.J., B.O., T.M.P.); and Research and Development Laboratories, N.V. Organon, Oss, The Netherlands (H.J.K.)

ABSTRACT

Tibolone is used to treat climacteric complaints and prevent osteoporosis. These beneficial effects are exerted via its 3α- and 3β-hydroxymetabolites. Undesirable stimulation of the breast and endometrium is not apparent. Endometrial stimulation is prevented by the progestogenic activity of its Δ^4-ene metabolite. The enzymes responsible for the formation of these active metabolites are unknown. Human aldo-keto reductase (AKR)1C isoforms have been shown to act as 3α/3β-hydroxysteroid dehydrogenases (HSDs) on 5α-dihydrotestosterone (5α-DHT). We show that AKR1Cs also efficiently catalyze the reduction of the $\Delta^{5(10)}$-3-ketosteroid tibolone to yield 3α- and 3β-hydroxytibolone. Homogeneous recombinant AKR1C1, AKR1C3, and AKR1C4 gave similar catalytic profiles to those observed with 5α-DHT. AKR1C1 catalyzed exclusively the formation of 3β-hydroxytibolone, AKR1C3 showed weak 3β/3α-HSD activity, and AKR1C4 acted predominantly as a 3α-HSD. Whereas AKR1C2 acted as a 3α-HSD toward 5α-DHT, it functioned exclusively as a 3β-HSD on tibolone. Furthermore, strong substrate inhibition was observed for the AKR1C2 catalyzed reduction of tibolone. Using NAD^+, the 3-hydroxymetabolites were efficiently oxidized by homogeneous recombinant AKR1C2 and AKR1C4. However, because of potent inhibition of this activity by NADPH, AKR1Cs will probably act only as 3-ketosteroid reductases in vivo. Molecular docking simulations using crystal structures of AKR1C1 and AKR1C2 explained why AKR1C2 inverted its stereospecificity from a 3α-HSD with 5α-DHT to a 3β-HSD with tibolone. The preference for AKR1C1 and AKR1C2 to form 3β-hydroxytibolone, and the preference of the liver-specific AKR1C4 to form 3α-hydroxytibolone, may explain why 3β-hydroxytibolone is the major metabolite in human target tissues and why 3α-hydroxytibolone is the major circulating metabolite.

Tibolone (Livial; [7α,17α]-17-hydroxy-7-methyl-19-norpregn-5(10)-en-20-yn-3-one) is a hormone replacement therapeutic used in the treatment of climacteric complaints and the prevention of osteoporosis (Albertazzi et al., 1998; Moore, 1999), but it may not stimulate the breast and endometrium (Colacurci et al., 1998; Valdivia and Ortega, 2000; Volker et al., 2001; Gompel et al., 2002; Blok et al., 2003). The agent has been assigned as a selective tissue estrogenic activity regulator (STEAR) to distinguish it from a selective estrogen receptor modulator (SERM) because its effects are not solely mediated by the estrogen receptor (Kloosterboer and Ederveen, 2003; Smith and O'Malley, 2004).

Tibolone exerts its tissue-specific effects via site-specific metabolism into three active derivatives: a 3α- and a 3β-hydroxy metabolite, and a Δ^4-isomer (Scheme 1) (Kloosterboer, 2001; Kloosterboer and Ederveen, 2003). Tibolone and its Δ^4-isomer are agonists for the androgen and progesterone receptors, whereas the two 3-hydroxymetabolites are weak ligands for the estrogen receptors (de Gooyer et al., 2003). In addition, tibolone and its 3-hydroxyderivatives inhibit estrogen sulfatase and reductive 17β-HSD isoforms (that convert estrone to 17β-estradiol) and activate oxidative 17β-HSD isoforms (that convert 17β-estradiol to estrone) in breast cancer cell lines (Chetrite et al., 1999; Pasqualini and Chetrite, 1999; Gompel et al., 2002; Purohit et al., 2002; van de Ven et al., 2002). These actions may selectively deprive the estrogen receptors in breast tissue of their natural ligands. A similar phenomenon is not seen in osteoblast-like cells (de Gooyer et al., 2001). Therefore, tissue-specific expression of

This work was supported by a sponsored research agreement from N.V. Organon (to T.M.P.)
Article, publication date, and citation information can be found at http://molpharm.aspetjournals.org.
doi:10.1124/mol.104.004515.

ABBREVIATIONS: AKR, aldo-keto reductase; HSD, hydroxysteroid dehydrogenase; 5α-DHT, 5α-dihydrotestosterone; TLC, thin layer chromatography; CV, coefficient of variation; PDB, Protein Data Bank; NSAID, nonsteroidal anti-inflammatory drug.

enzymes involved in tibolone activation may contribute to the selective actions of the drug. However, the human enzymes responsible for tibolone activation have not been identified.

After oral administration to women, tibolone is quickly metabolized into 3α- and 3β-hydroxytibolone (presumably in the intestine and liver). The plasma half-life of the two hydroxymetabolites is 7 h (Timmer et al., 2002), and the major phase I metabolite in the circulation is 3α-hydroxytibolone (Vos et al., 2002). Reduction of the 3-keto-moiety of tibolone is a prerequisite for the formation of sulfate conjugates at the C3 and C17 hydroxy groups (Vos et al., 2002) via phase II sulfotransferases. In addition, minor amounts of the Δ^4-isomer of tibolone were also found in the circulation, but no half-life was estimated. In contrast to the circulating metabolites, tibolone is converted in peripheral human target tissues (e.g., uterus and vagina) to the 3β-hydroxy metabolite (Blom, 2001). Formation of minor amounts of the Δ^4-isomer was also observed in these target tissues. The formation of the 3β-hydroxy metabolite as well as the Δ^4-isomer were expected to be catalyzed by NAD(H)-dependent 3β-HSD/Δ^{5-4} ketosteroid isomerase (3β-HSD/ketosteroid isomerase). However, the formation of 3β-hydroxytibolone was NADPH-dependent and could not be inhibited by the 3β-HSD/ketosteroid isomerase inhibitor epostane (Blom, 2001), and the formation of the Δ^4-isomer was neither cofactor-dependent nor could it be inhibited by epostane (Blom, 2001), suggesting other routes to their formation.

The four cytosolic enzymes of the AKR1C subfamily in the aldo-keto reductase (AKR) superfamily [i.e., human 20α-HSD (AKR1C1), human 3α-HSD type 3 (AKR1C2; also known as bile acid binding protein), human 3α-HSD type 2 (AKR1C3; also known as human 17β-HSD type 5), and human 3α-HSD type 1 (AKR1C4) (Penning, 1997)] act as non-positional-specific 3α-/17β-/20α-HSDs (Penning et al., 2000). This means that in vitro the isoforms catalyzed the bidirectional interconversion of 3-ketosteroids and 3α-hydroxysteroids, 17-ketosteroids and 17β-hydroxysteroids, and 20-ketosteroids and 20α-hydroxysteroids to varying extents. AKR1C1-AKR1C4 also act as 3β-HSDs and catalyze the reduction of the fully saturated 3-ketosteroid 5α-DHT into 3α- and 3β-androstanediol (Steckelbroeck et al., 2004). The ratio of reductive 3α-HSD versus 3β-HSD activity varied significantly among the isoforms in a way that AKR1C1 had to be considered as a predominant 3β-HSD, AKR1C2 as an almost exclusive 3α-HSD, AKR1C3 as a weak 3α/3β-HSD, and AKR1C4 as a predominant 3α-HSD. AKR1C4 expression is apparently liver-specific, whereas mRNA expression of the other three isozymes was observed in a variety of human tissues displaying tissue-specific patterns (Penning et al., 2000). The catalytic properties of these proteins together with their tissue-specific expression patterns suggested that the AKR1C isozymes could be responsible for the formation of both the 3α-hydroxy- and the 3β-hydroxy metabolite of tibolone.

We now demonstrate that recombinant homogeneous AKR1C1-AKR1C4 catalyze the 3-ketosteroid reduction of tibolone into 3α- and 3β-hydroxytibolone. We find that AKR1C2 inverted its stereospecificity from a 3α-HSD with 5α-DHT to a 3β-HSD with tibolone. This represents a unique example where an HSD can invert its stereospecificity in a substrate-dependent manner. The preference of AKR1C1 and AKR1C2 to form 3β-hydroxytibolone and the liver-specific AKR1C4 to form 3α-hydroxytibolone may account for the metabolic profile of the drug.

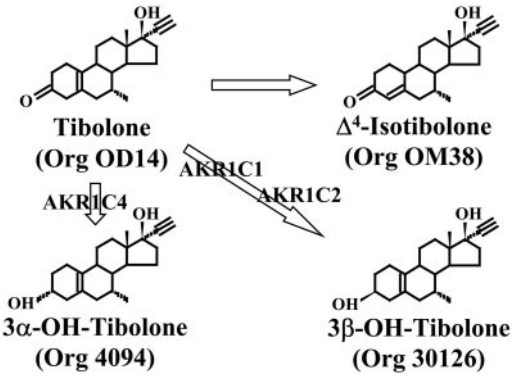

Scheme 1. The three active metabolites of tibolone: ([7α,17α]-17-hydroxy-7-methyl-19-norpregn-5(10)-en-20-yn-3-one; Org OD14); 3α- and 3β-OH-tibolone ([3α/3β,7α,17α]-3,17-dihydroxy-7-methyl-19-norpregn-5(10)-en-20-yn-3-one; Org 4094 and Org30126); and Δ^4-isotibolone ([7α,17α]-17-hydroxy-7-methyl-19-norpregn-4(5)-en-20-yn-3-one; Org OM38).

Materials and Methods

Steroids and Chemicals. Tibolone (Org OD14), 3α- and 3β-hydroxytibolone ([3α- or 3β,7α,17α]-3,17-dihydroxy-7-methyl-19-norpregn-5(10)-en-20-yn-3-one; Org 4094 and Org30126, respectively), Δ^4-isotibolone ([7α,17α]-17-hydroxy-7-methyl-19-norpregn-4(5)-en-20-yn-3-one, Org OM38), [16-^{3}H]tibolone (32.8 Ci/mmol) [16-^{3}H]3α-hydroxytibolone (38.0 Ci/mmol) and [16-^{3}H]3β-hydroxytibolone (34.4 Ci/mmol) were obtained from N.V. Organon (Oss, The Netherlands). Flufenamic acid was obtained from MP Biomedicals (Aurora, OH). Pyridine nucleotides were purchased from Roche Diagnostics (Indianapolis, IN). All other reagents were of American Chemical Society grade or better.

Substrate Titration. Stock solutions of tibolone were prepared in acetonitrile. To determine the concentration of these stock solutions, we developed a titration assay based on the absorbance of the Δ^4-isotibolone chromophore at 248 nm (ϵ = 17,000 M^{-1} cm^{-1}). Tibolone was converted into Δ^4-isotibolone in a base-catalyzed reaction by adding 75 μl of a 1 M solution of NaOH to a mixture of 920 μl of 10 mM potassium phosphate, pH 7.0, and 5 μl of the tibolone stock solution. Formation of Δ^4-isotibolone was monitored spectrophotometrically until the reaction reached its endpoint.

Expression and Purification of Recombinant Human AKR1C Isoforms. Recombinant human AKR1C isoforms were overexpressed in *Escherichia coli* C41(DE3) host cells transformed with the inducible prokaryotic expression vectors pET-16b as described previously (Burczynski et al., 1998; Ratnam et al., 1999). Recombinant enzymes were purified to homogeneity from bacterial sonicates by sequential chromatography on a DE52 anion exchange and a Sepharose Blue column according to a previously described protocol (Burczynski et al., 1998) to yield enzymes of the following specific activities: 0.21 μmol of androsterone (75 μM) oxidized per minute per milligram (AKR1C4) and 2.1, 2.5, and 2.8 μmol of 1-acenaphthenol (1 mM) oxidized per minute per milligram (AKR1C1, AKR1C2, and AKR1C3, respectively). Purity of the enzymes was verified by SDS-polyacrylamide gel electrophoresis, and protein concentration was determined (Bradford, 1976). The homogeneous enzymes were stored in aliquots at −80°C.

Radiometric Assays. Standard incubations (final volume of 100 μl) were conducted in 100 mM potassium phosphate buffer, pH 7.0, with 5% acetonitrile containing 200,000 dpm [16-^{3}H]-steroid and unlabeled steroid to obtain the final substrate concentration. Purified enzymes were added and the reactions were started by the addition of coenzyme. Assays were incubated at 37°C (time-course

analyses) or 25°C (all other experiments), and the reactions were terminated by the addition of 750 μl of ice-cold water-saturated ethyl acetate. Steroids were extracted by continuous vortexing for 5 min, the organic phases were transferred into glass tubes and the extraction step was repeated once. The combined organic phases were evaporated to complete dryness.

The dried extracts were redissolved in 50 μl of acetonitrile and applied to LK6D Silica TLC plates (Whatman, Clifton, NJ). Remaining residues of the extracts were redissolved in 50 μl of chloroform/ethanol [35:15 (v/v)] containing 25 μg each of nonradioactive reference steroids: tibolone, Δ^4-isotibolone, and 3α- and 3β-hydroxytibolone. These mixtures were then applied to the LK6D Silica TLC plates on top of the corresponding first spot. The chromatograms were developed in dichloromethane/acetone [92.5:7.5 (v/v)]. The linear radiodistribution on the TLC plates was scanned with an automatic TLC-linear analyzer (Bioscan Imaging Scanner System 200-IBM with AutoChanger 3000; Bioscan, Washington, DC). Computer-aided quantitative evaluation of radiosignals emitted from the plates permitted calculation of the relative amount of each radioactive steroid as a percentage of the total radioactivity recovered from a single TLC lane. Blank values were subtracted. The positions of radioactive steroid signals on the TLC plates were verified by staining of cochromatographed reference standards as described previously (Steckelbroeck et al., 2004). The coefficient of variation (i.e., the standard deviation expressed as a percentage of the mean) of the assay was determined from sets of 10 measurements for each 1 and 10 μM final tibolone concentration. The CVs for the formation of the major AKR1C4 product 3α-hydroxytibolone were 2.0 and 2.7%, respectively. The CVs for the formation of the minor product 3β-hydroxytibolone were 5.5 and 7.9%, respectively. Similar CVs were observed with the other AKR1C isoforms. For autoradiography analysis, the TLC-plates were exposed to X-ray film for 1 week at −70°C.

Spectrophotometric Assays. Spectrophotometric analyses of the reduction of tibolone were performed at 25°C and pH 7.0 as described previously (Penning et al., 2000) by monitoring the decrease in NADPH absorbance at 340 nm on a DU 640 spectrophotometer (Beckman Coulter, Fullerton, CA).

Spectrofluorometric Assays. Spectrofluorometric analyses of the reduction of tibolone were performed by monitoring the decrease in NADPH emission on a fluorescence spectrophotometer F-4500 (Hitachi America, Ltd., New York, NY). Assays were conducted at 25°C in 100 mM potassium phosphate buffer, pH 7.0, at a final volume of 1 ml containing 5% acetonitrile. The reaction was initiated by the addition of enzyme. The oxidation of NADPH was measured by monitoring the decrease of fluorescence emission of NADPH at 450 nm (slit-width 10 mm) with excitation at 340 nm (slit-width 10 mm). A standard curve was constructed on a daily basis, which monitored the ΔF at 450 nm upon incremental addition of NADPH. This curve permitted the rates of fluorescence change to be calculated as nanomoles of NADPH oxidized per minute (Lowry and Passonneau, 1972).

Determination of Steady-State Kinetic Parameters. K_M and k_{cat} values for the reduction of tibolone by AKR1C2 and AKR1C9 were determined in the continuous spectrofluorometric assays and continuous spectrophotometric assay, respectively. K_M and k_{cat} values for the reduction of tibolone by AKR1C1 and AKR1C4 were also determined in a discontinuous radiometric assay. In this assay, data from three different time points were analyzed via nonlinear curve fitting with the Fig. P 2.7 program for Windows (Biosoft, Cambridge, UK) using the equation for pseudofirst order decay: $[P]_t = [S] \times (1 - e^{-kt})$. Kinetic analyses of initial velocities obtained were performed using the Henri-Michaelis-Menten equation $[V]_t = V_{max} \times [S]_0/(K_M + [S]_0)$. Kinetic analyses of the initial velocities of AKR1C2 were conducted using an equation for substrate inhibition: $[V]_t = V_{max}/(1 + K_M/[S]_0 + [S]_0/K_{iapp})$, where K_{iapp} represents the dissociation constant for the presumed inhibitory SES complex, where two molecules of tibolone are bound and NADPH is held constant at saturating concentrations.

The k_{catapp} values for 3-hydroxytibolone oxidation catalyzed by AKR1C isoforms were calculated using the exact molecular weight of the AKR1C isoforms to convert specific enzyme activities obtained from radiometric time courses. Specific enzyme activities were calculated by determination of the tangents to the linear part of the exponential fit of the untransformed progress curve observed at maximal achievable substrate concentrations.

Molecular Docking Simulations. Simulations of tibolone binding into the active sites of AKR1C1 and AKR1C2 were performed using the AutoDock program (version 3.0) (Morris et al., 1998) as described previously (Steckelbroeck et al., 2004). Coordinates of AKR1C1 and AKR1C2 taken from Protein Data Bank (PDB) entries 1MRQ (Couture et al., 2003) and 1IHI (Jin et al., 2001) were used as the starting structures for the docking of the steroid molecule into AKR1C1 and AKR1C2, respectively. Existing solvent molecules and steroid ligands were removed to generate docking targets containing one molecule of the respective enzyme and the NADPH cofactor with a bent nicotinamide ring (PDB entry 1HET) overlaid onto the original $NADP^+$ position. N.V. Organon kindly provided the crystallographic coordinates of tibolone. The starting position of tibolone for docking simulations was >30 Å away from the center of the steroid binding cavities. Docking computations were performed using the Lamarckian genetic algorithm and simulated annealing protocols. Each protocol consisted of 256 runs, with each run producing a docked conformer. Cluster analysis was performed which grouped the conformers with root-mean-square deviation in atomic positions of less than 1.0 Å into one cluster and ranked clusters by docking energy.

Results

Tibolone Reduction Catalyzed by AKR1C Isoforms. To determine whether the four human AKR1C isoforms could catalyze the 3-ketosteroid reduction of the synthetic $\Delta^{5(10)}$-19-nor-3-ketosteroid tibolone and to address the stereospecificity of the reactions, the metabolism of the drug by these enzymes was investigated. The experiments revealed that recombinant homogeneous AKR1Cs catalyzed the NADPH-dependent reduction of tibolone. AKR1C1 and AKR1C2 generated a single tibolone product that comigrated with the authentic 3β-hydroxytibolone standard, whereas AKR1C3 and AKR1C4 produced two products, one comigrating with the authentic 3α-hydroxytibolone and one with the authentic 3β-hydroxytibolone (Fig. 1). Related rat liver AKR1C9 generated a single product, which comigrated with the 3α-hydroxytibolone standard.

Using 20 μM tibolone and 2.3 mM NADPH, we observed notable differences in 3α- and/or 3β-hydroxytibolone formation over time catalyzed by the various recombinant homogeneous human AKR1C isoforms (Fig. 2). AKR1C1 and AKR1C2 exclusively catalyzed the formation of 3β-hydroxytibolone. In contrast, AKR1C4 predominantly catalyzed the formation of 3α-hydroxytibolone. AKR1C3 showed low 3-ketosteroid reductase activity toward tibolone, in which the enzyme formed higher amounts of 3β-hydroxytibolone than 3α-hydroxytibolone.

Evidence That 3α- and 3β-Hydroxytibolone Formation Occurs at the Same Active Site. Nonsteroidal anti-inflammatory drugs (NSAIDs) are known to competitively inhibit AKR1Cs (Penning and Talalay, 1983). To substantiate that 3α- and 3β-hydroxytibolone formation by AKR1C3 and AKR1C4 occur at the same active site, we exploited our previous observation that reduction of 5α-DHT via the 3α- and 3β-HSD activity of the human AKR1C isoforms was inhibited by the NSAID flufenamic acid (Steckelbroeck et al., 2004).

We investigated the effects of increasing flufenamic acid concentrations on the reduction of 1 μM tibolone catalyzed by the various recombinant human isoforms. Dose-dependent inhibition of tibolone reduction was observed for all AKR1C isoforms (Fig. 3). Formation of 3α- and of 3β-hydroxytibolone by AKR1C3 and AKR1C4 were both sensitive to inhibition by the NSAID. The IC_{50} values for the formation of 3α- and 3β-hydroxytibolone were 2.6 and 2.3 μM in AKR1C3, and >1000 μM and >1000 μM in AKR1C4, respectively. The similarity in the inhibition curves for the two reactions on both AKR1C3 and AKR1C4 is consistent with these reactions taking place at the same active site of each enzyme. The IC_{50} values for the formation of 3β-hydroxytibolone in AKR1C1 and AKR1C2 were 0.9 and 0.6 μM, respectively.

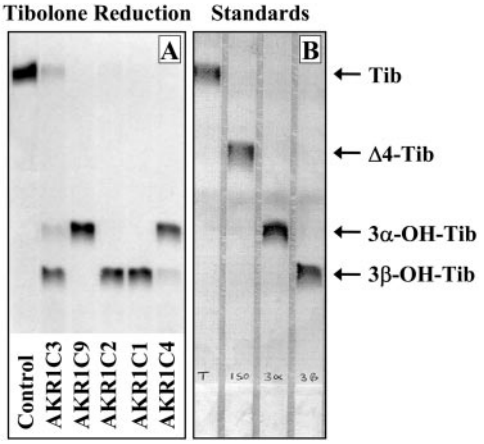

Fig. 1. Human AKR1C isoforms reduce tibolone into 3α- and 3β-hydroxytibolone. Autoradiograms of TLC analyses of the NADPH-dependent reduction of 20 μM [^{3}H]tibolone. A, incubations of no enzyme control (100 min), homogeneous recombinant AKR1C3 (100 min), homogeneous recombinant AKR1C9 (30 min), homogeneous recombinant AKR1C2 (30 min), homogeneous recombinant AKR1C1 (60 min), and homogeneous recombinant AKR1C4 (30 min). B, photograph of the cochromatographed and stained nonradioactive standards: tibolone (Tib), Δ^4-isotibolone (Δ^4-Tib), and 3β/3α-hydroxytibolone (3β/3α-OH-Tib). Radiometric assays were performed with 2.3 mM NADPH at pH 7.0 and 37°C as described under *Materials and Methods*. Chromatograms were exposed to X-ray film at −70°C for 1 week.

Steady-State Kinetic Parameters of the Reduction of Tibolone by AKR1C1 Isoforms. To determine the kinetic constants of tibolone reduction by the human AKR1C isoforms, initial velocities were determined at varying tibolone concentrations in 1) noncontinuous radiometric assays using 100 μM NADPH and 2) continuous spectrofluorometric assays using 7 μM NADPH. Steady-state kinetic parameters for the reduction of tibolone by rat liver AKR1C9 were determined in continuous spectrophotometric assays with 180 μM NADPH as a control. Nonlinear curve-fitting analyses yielded k_{cat} and K_M values and their standard errors of mean (Fig. 4; Table 1). An apparent substrate inhibition was observed for the AKR1C2-catalyzed reaction. Fitting the initial velocity data according to a presumed inhibitory SES complex yielded a K_{iapp} value for the inhibition of AKR1C2 by the substrate tibolone (Table 1).

Depending on the assay used, a 5-fold difference in k_{cat} but not in K_M was observed (Table 1). To exclude that these differences were based on different coenzyme concentrations in the radiometric versus the spectrofluorometric assays, kinetic constants of AKR1C1 were redetermined in a radiometric assay using 8 μM instead of 100 μM NADPH. Identical k_{cat} values were observed, which ruled out that different coenzyme concentrations were responsible for the differences in k_{cat}. Because continuous spectrofluorometric assays are likely to be more accurate, we focus our attention on these values.

Examination of the bimolecular rate constants for the reduction of tibolone was revealing (Fig. 4; Table 1). First, with rat AKR1C9 5α-DHT (k_{cat}/K_M value of 26,000 min^{-1} mM^{-1}; V. V. Heredia, unpublished data) is a slightly superior substrate to tibolone (k_{cat}/K_M value of 16,791 min^{-1} mM^{-1}).

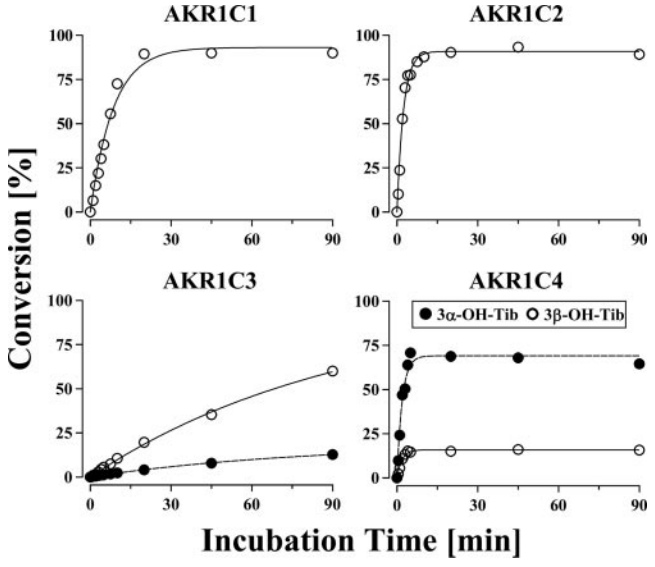

Fig. 2. Time courses of the NADPH-dependent reduction of tibolone into 3α- and 3β-hydroxytibolone catalyzed by human AKR1C isoforms. Conversion of 20 μM [^{3}H]tibolone into 3α-hydroxytibolone (●) and 3β-hydroxytibolone (○) by homogeneous recombinant AKR1C1 (5 μg), AKR1C2 (6.2 μg), AKR1C3 (5.8 μg), and AKR1C4 (9 μg). The results represent mean values of radiometric assays performed in duplicate with 2.3 mM NADPH at pH 7.0 and 37°C as described under *Materials and Methods*.

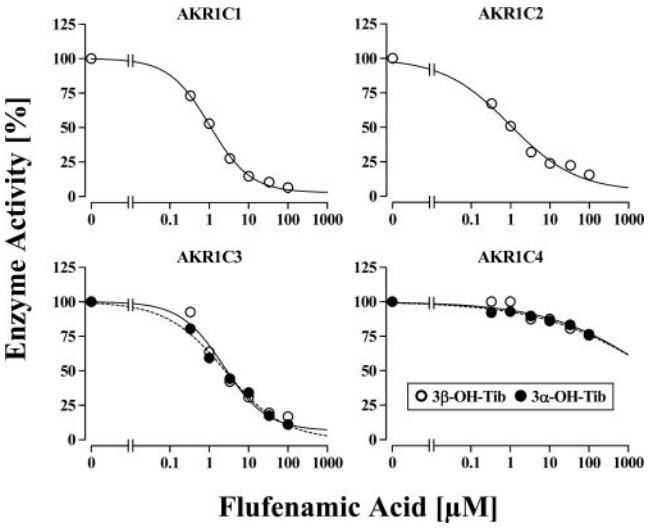

Fig. 3. Reduction of tibolone into 3α- and 3β-hydroxytibolone catalyzed by human AKR1C isoforms is inhibited by the NSAID flufenamic acid. The NADPH-dependent reduction of 1 μM [^{3}H]tibolone into 3α-hydroxytibolone (●) and 3β-hydroxytibolone (○) by homogeneous recombinant AKR1C1, AKR1C2, AKR1C3, and AKR1C4 was investigated in the presence of increasing flufenamic acid concentrations. The results represent mean values of radiometric assays performed in duplicate with 2.3 mM NADPH at pH 7.0 and 25°C as described under *Materials and Methods*.

Second, AKR1C1, AKR1C2, and AKR1C4 efficiently catalyzed the reduction of tibolone with significantly higher k_{cat}/K_M values (1158–14,348 min^{-1} mM^{-1}) than those reported for the reduction of 5α-DHT. The previously published values for the reduction of 5α-DHT were 8 min^{-1} mM^{-1} for AKR1C1 (where the radiometric assay did not distinguish between the formation of 3α- and 3β-androstanediol; Penning et al., 2000), and 714 min^{-1} mM^{-1} for AKR1C2 and 586 min^{-1} mM^{-1} for AKR1C4 (where the spectrophotometric assays did not distinguish between the formation of 3α- and 3β-androstanediol; Penning et al., 2000; Steckelbroeck et al., 2004). Third, AKR1C2 had a k_{cat}/K_M value for the reduction of tibolone, which exceeds the value of AKR1C4 by almost an order of magnitude. By contrast, AKR1C1 had a more modest k_{cat}/K_M value than AKR1C4. Because of low enzyme activity, kinetic parameters for the AKR1C3-catalyzed reaction could not be determined without violating steady-state conditions.

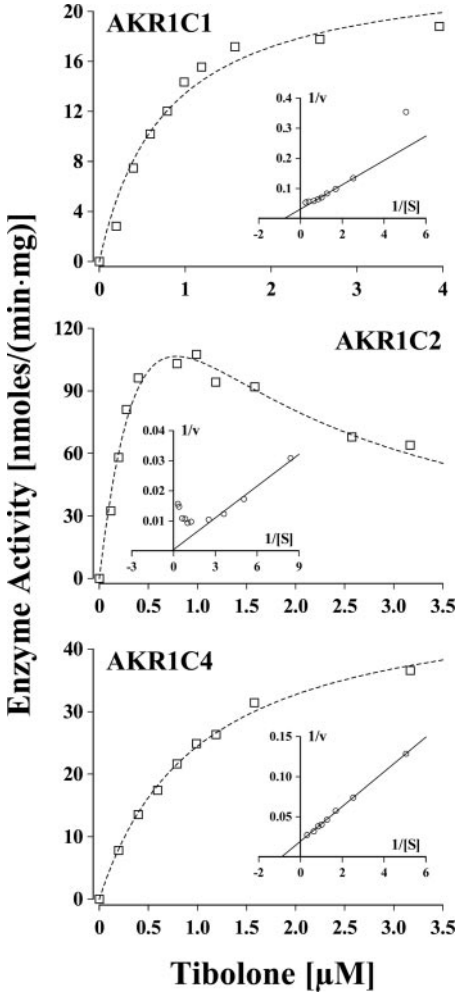

Fig. 4. Michaelis-Menten kinetics for the reduction of tibolone by AKR1C isoforms. Initial velocities of tibolone reduction were measured fluorimetrically using different substrate concentrations with 7 μM NADPH at 25°C and pH 7.0. The results represent mean values of incubations performed in duplicate with homogeneous recombinant AKR1C1, AKR1C2, and AKR1C4 as described under *Materials and Methods*. Plots of initial velocity versus substrate concentration were drawn by nonlinear curve fitting analysis. The insets show the respective double reciprocal plots.

3α- and 3β-Hydroxytibolone Oxidation Catalyzed by Human AKR1C Isoforms. AKR1C isoforms expressed substantial in vitro 3α[17β]-hydroxysteroid oxidase activity toward 3α-androstanediol (Steckelbroeck et al., 2004). We also determined whether recombinant homogeneous AKR1C1s express NAD^+-dependent hydroxysteroid oxidase activity toward 3α- and 3β-hydroxytibolone, respectively. Substantial oxidative enzyme activity was observed for AKR1C2 and AKR1C4 (Fig. 5). AKR1C2 catalyzed the oxidation of 3β-hydroxytibolone to tibolone, and AKR1C4 catalyzed the oxidation of both substrates.

Time-course analyses with 20 μM substrate and 2.3 mM NAD^+ revealed that homogeneous recombinant AKR1C1 and AKR1C3 functioned as poor 3β-hydroxysteroid oxidases, whereas AKR1C2 functioned as an efficient 3β-hydroxysteroid oxidase (Fig. 6). AKR1C4 not only acted as efficient 3α/3β-hydroxysteroid oxidase to form tibolone but also as an epimerase to convert 3β-hydroxytibolone into 3α-hydroxytibolone and vice versa. This suggests that, in vitro, epimerization occurs via tibolone as the intermediate using AKR1C4-generated NADH as reducing cofactor. A summary of k_{catapp} values and specific activities for 3α/3β-hydroxytibolone oxidation catalyzed by the AKR1C isoforms is given in Table 2.

Influence of the NADPH/NAD^+ Ratio on the Oxidation of 3-Hydroxytibolone by the AKR1C Isoforms. We have previously shown that, in vitro, the NAD^+-dependent 3α[17β]-hydroxysteroid oxidase activity of the AKR1C isoforms toward 3α/3β-androstanediol was potently inhibited by low micromolar NADPH concentrations, whereas their NADPH-dependent 3-ketosteroid reductase activity toward 5α-DHT was not inhibited by the opposing cofactor NAD^+ (Steckelbroeck et al., 2004). To determine whether the

TABLE 1

Kinetic parameters for 3-ketosteroid reduction of tibolone catalyzed by homogeneous recombinant AKR1C isoforms

Kinetic parameters were determined radiometrically (R), fluorimetrically (F), or spectrophotometrically (S). The K_{iapp} value reflects significant substrate inhibition observed when AKR1C2 activity was investigated. Radiometric analyses of AKR1C4 revealed kinetic parameters for the reduction of tibolone to 3α-hydroxytibolone (3α-OH-Tib) and 3β-hydroxytibolone (3β-OH-Tib). Assays were performed in duplicate at pH 7.0 and 25°C as described under *Materials and Methods*.

Enzyme	K_M	k_{cat}	k_{cat}/K_M	K_{iapp}
	μM	*min^{-1}*	*min^{-1} mM^{-1}*	*μM*
AKR1C1 (R, 100 μM NADPH)	1.09 ± 0.14	0.15 ± 0.01	136	
AKR1C1 (R, 8 μM NADPH)	1.23 ± 0.19	0.15 ± 0.01	122	
AKR1C1 (F, 7 μM NADPH)	0.76 ± 0.13	0.88 ± 0.06	1158	
AKR1C2 (F, 7 μM NADPH)	0.87 ± 0.34	12.7 ± 3.7	14348	0.70 ± 0.29
AKR1C3	N.D.	N.D.	N.D.	
AKR1C4 [3α-OH-Tib] (R, 100 μM NADPH)	1.06 ± 0.09	0.28 ± 0.01	268	
AKR1C4 [3β-OH-Tib] (R, 100 μM NADPH)	0.95 ± 0.09	0.06 ± < 0.01	66	
AKR1C4 (F, 7 μM NADPH)	1.02 ± 0.07	1.83 ± 0.06	1794	
AKR1C9 (S, 180 μM NADPH)	4.82 ± 0.55	85.8 ± 4.1	16,791	

N.D., not detectable.

AKR1C isoforms behave similarly with the synthetic $\Delta^{5(10)}$-steroids, we investigated the influence of the NADPH/NAD^+ ratio on 1) the in vitro 3-ketosteroid reductase activity of the AKR1Cs toward tibolone and 2) the in vitro 3α/3β-hydroxysteroid oxidase activity of the AKR1Cs toward 3α/3β-hydroxytibolone, respectively. NADPH-dependent 3-ketosteroid reductase activity of the enzymes was not inhibited by equal concentrations of NAD^+ (Fig. 7A; 1 mM NADPH plus 1 mM NAD^+ final concentrations), whereas NAD^+-dependent hydroxysteroid oxidase activity of the enzymes was potently inhibited by low micromolar concentrations of NADPH (Fig. 7B; 1 mM NAD^+ plus 0.01 mM NADPH final concentrations).

Molecular Docking Simulations to Identify the Preferred Position of Tibolone in the Active Sites of AKR1C1 and AKR1C2. We have previously validated a molecular modeling approach to simulate the docking of steroid ligands into the active sites of AKR1C1 and AKR1C2 using crystal structures of the two isoforms (Steckelbroeck et al., 2004). To explain why AKR1C2 inverted its stereospecificity from a 3α-HSD with 5α-DHT to a 3β-HSD with tibolone, and why AKR1C1 retained its stereospecificity as a 3β-HSD with both 5α-DHT and tibolone, we performed molecular docking simulations.

Tibolone was bound in a similar manner in the active sites of both AKR1C1 and AKR1C2 (Fig. 8A). When it was docked into AKR1C1, the conformation in the cluster with the lowest energy (E_D = −9.2 kcal/mol) was found 237 times of 256 runs and represented a binding orientation that explains the formation of 3β-hydroxytibolone. The C3-ketone of the steroid is in proximity to the C4 of nicotinamide (3.6 Å), and the α-face of the steroid is directed toward the 4-*pro*-R hydrogen for hydride transfer. It is interesting that, when tibolone was docked to AKR1C2 all clusters had similar docking energies (E_D = −9.0 to −8.6 kcal/mol). The second ranked conformation (found 4 times of 256 runs) had a docking energy of 0.4 kcal/mol greater than the top ranked cluster and depicts the positional arrangement between tibolone and the cofactor for

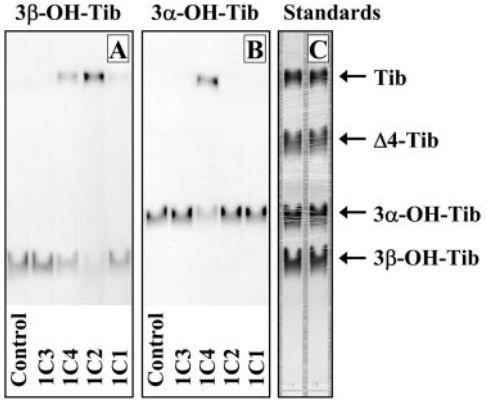

Fig. 5. Human AKR1C isoforms oxidize 3α- and 3β-hydroxytibolone. Autoradiograms of TLC analyses. A, NAD^+-dependent oxidation of 20 μM [^{3}H]3β-hydroxytibolone (3β-OH-Tib). B, NAD^+-dependent oxidation of 20 μM [^{3}H]3α-hydroxytibolone (3α-OH-Tib). Incubations of no enzyme control (60 min), homogeneous recombinant AKR1C3 (60 min), homogeneous recombinant AKR1C4 (15 min), homogeneous recombinant AKR1C2 (30 min), and homogeneous recombinant AKR1C1 (60 min). C, photograph of the cochromatographed and stained nonradioactive standards: tibolone (Tib), Δ^4-isotibolone (Δ^4-Tib), and 3β/3α-hydroxytibolone (3β/3α-OH-Tib). Radiometric assays were performed with 2.3 mM NAD^+ at pH 7.0 and 37°C as described under *Materials and Methods*. Chromatograms were exposed to X-ray film at −70°C for 1 week.

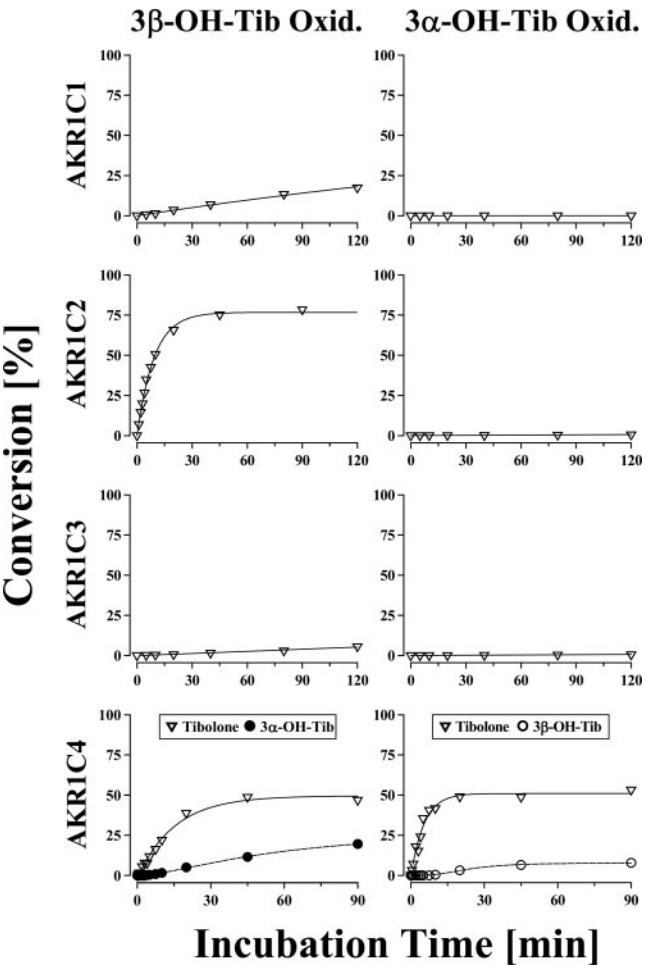

Fig. 6. Time courses of the NAD^+-dependent oxidation of 3α- and 3β-hydroxytibolone into tibolone catalyzed by human AKR1C isoforms. Left, conversion of 20 μM [^{3}H]3β-hydroxytibolone into tibolone (▽) and 3α-hydroxytibolone (●) by homogeneous recombinant AKR1C1 (5 μg), AKR1C2 (6.2 μg), AKR1C3 (5.8 μg), and AKR1C4 (9 μg). Right, conversion of 20 μM [^{3}H]3α-hydroxytibolone into tibolone (▽) and 3β-hydroxytibolone (○) by homogeneous recombinant AKR1C1, AKR1C2, AKR1C3, and AKR1C4. The results represent mean values of radiometric assays performed in duplicate with 2.3 mM NADPH at pH 7.0 and 37°C as described under *Materials and Methods*.

TABLE 2

NAD^+-dependent oxidation of 3β-hydroxytibolone (3β-OH-Tib) and 3α-hydroxytibolone (3α-OH-Tib) to tibolone by homogeneous recombinant human AKR1C1-AKR1C4 isoforms

Specific activities and k_{catapp} values were obtained from time-course analyses for the oxidation of 20 μ M [^{3}H]3α/3β-Hydroxytibolone with 2.3 mM NAD^+ at pH 7.0 and 37°C as described under *Materials and Methods*.

Substrate	Specific Activity	k_{catapp}
	nmol min^{-1} mg^{-1}	*min^{-1}*
AKR1C1		
3β-OH-Tib	0.79	0.03
3α-OH-Tib	0	0
AKR1C2		
3β-OH-Tib	25.3	0.94
3α-OH-Tib	0.02	<0.01
AKR1C3		
3β-OH-Tib	0.15	<0.01
3α-OH-Tib	0.02	<0.01
AKR1C4		
3β-OH-Tib	6.53	0.24
3α-OH-Tib	18.8	0.69

the formation of 3β-hydroxytibolone. The C3-ketone group is 3.5 Å away from the C4 of nicotinamide and the α-face of the steroid is directed to the 4-*pro*-R hydrogen. All other AKR1C2 conformations seemed to be nonproductive binding modes where the C3-ketone group of the steroid was distant from the cofactor (>8 Å).

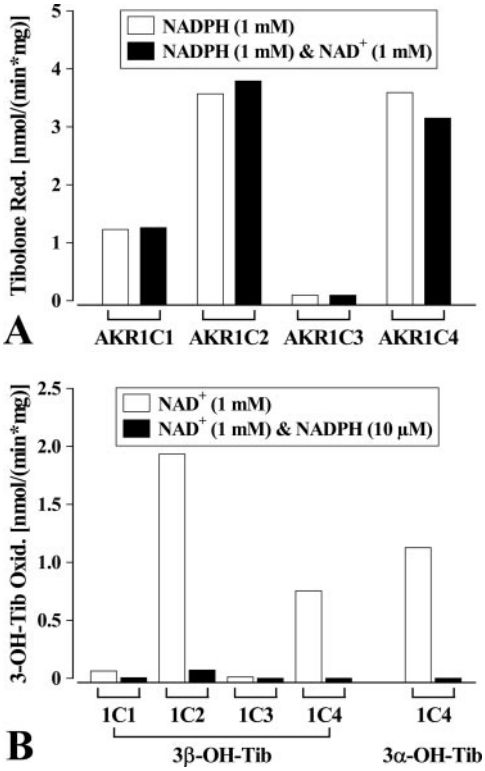

Fig. 7. NADPH is a potent inhibitor of the NAD^+-dependent oxidation of 3α- and 3β-hydroxytibolone catalyzed by homogeneous recombinant human AKR1C isoforms. A, inhibitory effects of NAD^+ on the NADPH-dependent reduction of 1 μM [^{3}H]tibolone by homogeneous recombinant AKR1C1-AKR1C4 were investigated using either 1 mM NADPH alone (open columns) or 1 mM NADPH and 1 mM NAD^+ in combination (filled columns). B, inhibitory effects of NADPH on the NAD^+-dependent oxidation of 1 μM [^{3}H]3β-hydroxytibolone (3β-OH-Tib) by AKR1C1-AKR1C4 and the NAD^+-dependent oxidation of 1 μM [^{3}H]3α-hydroxytibolone (3α-OH-Tib) by AKR1C4 were investigated using either NAD^+ alone (open columns) or 1 mM NAD^+ and 0.01 mM NADPH in combination (filled columns). The results represent mean values of radiometric assays performed in duplicate at pH 7.0 and 25°C as described under *Materials and Methods*.

Discussion

To date, no enzyme has been identified that could account for the bioactivation of tibolone to its active 3α- and 3β-hydroxymetabolites. These reactions occur in the liver and intestine as well as in tibolone target tissues and are essential for 1) the apparent tissue-specific actions of tibolone (Kloosterboer and Ederveen, 2003) and 2) the catabolic clearance of the drug (Timmer et al., 2002; Vos et al., 2002). We previously demonstrated that the four human AKR1C isoforms catalyze the reduction of 5α-DHT into 3α- and 3β-androstanediol (Steckelbroeck et al., 2004). Our present study shows that the recombinant homogeneous human AKR1C isoforms also catalyze the reduction of tibolone into 3α- and 3β-hydroxytibolone. This property and their tissue-specific expression patterns suggest that AKR1C isoforms are responsible for the formation of 3α- and 3β-hydroxytibolone in the liver and intestine as well as in tibolone target tissues in humans.

AKR1C1-AKR1C4 are known to catalyze the 3-ketosteroid reduction of fully saturated 3-ketosteroids such as 5α-DHT (Penning et al., 2000; Steckelbroeck et al., 2004). With 5α-DHT, AKR1C1 acted as a 3β-HSD with subsidiary 3α-HSD activity, AKR1C2 acted as an efficient 3α-HSD, AKR1C3 acted as a weak 3α/3β-HSD, and AKR1C4 acted an efficient 3α-HSD with subsidiary 3β-HSD activity (Scheme 1). We now show that the enzymes also catalyze the reduction of $\Delta^{5(10)}$-19-nor-3-ketosteroids such as tibolone (Fig. 1). With tibolone AKR1C1, AKR1C3 and AKR1C4 gave a similar catalytic profile to that observed with 5α-DHT (Fig. 1). Time-course analyses of tibolone reduction revealed that AKR1C1 functioned exclusively as a 3β-HSD, AKR1C3 functioned as a weak 3β/3α-HSD, and AKR1C4 functioned predominantly as an efficient 3α-HSD (Fig. 2; Scheme 1). However, whereas AKR1C2 acted as an efficient and almost exclusive 3α-HSD with 5α-DHT, it inverted its stereospecificity with tibolone and acted exclusively as a 3β-HSD. These striking results reveal a unique substrate-dependent switch in stereospecificity in steroid metabolism catalyzed by HSDs.

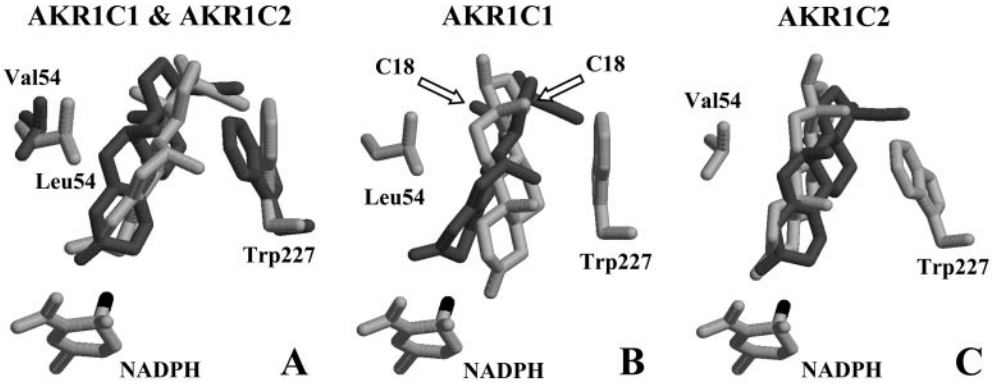

Fig. 8. Binding modes of tibolone versus 5α-DHT in the active sites of AKR1C1 and AKR1C2. A, superimposition of the preferred active docking positions of tibolone in binary complexes of AKR1C1-NADPH (light gray) and AKR1C2-NADPH (dark gray). B, superimposition of the preferred active docking positions of tibolone (dark gray) and 5α-DHT (light gray) in the AKR1C1-NADPH binary complex; the position of the angular C18 methyl group in both steroids is indicated. C, superimposition of the preferred active docking positions of tibolone (dark gray) and 5α-DHT (light gray) in the AKR1C2-NADPH binary complex. Details of docking simulations and PDB entry numbers are given under *Materials and Methods*. The 4-*pro*-R hydrogen of NADPH (shown in black) is directed to the α-face of tibolone in both AKR1C1 and AKR1C2 (3β-HSD reaction), whereas the 4-*pro*-R hydrogen of NADPH is directed to the α-face of 5α-DHT in AKR1C1 (3β-HSD reaction) and to the β-face of 5α-DHT in AKR1C2 (3α-HSD reaction).

The NSAID flufenamic acid is a competitive inhibitor of AKR1C enzymes (Penning and Talalay, 1983). We investigated the inhibition of AKR1C-catalyzed tibolone reduction by this NSAID to substantiate that 3α- and 3β-hydroxytibolone formation occurs at the same active site of AKR1C3 and AKR1C4. The formation of both 3α- and 3β-hydroxytibolone were equally sensitive to inhibition by low micromolar concentrations of the NSAID (Fig. 3.). This is consistent with the two reactions occurring at the same active site of the AKR1C isoforms. It is noteworthy that flufenamic acid only inhibits AKR1C4 at millimolar concentrations, suggesting that persons receiving NSAID therapy would not lack the bioactivation of tibolone to 3α- and 3β-hydroxytibolone in the liver.

When the bimolecular rate constants for tibolone reduction by the human AKR1C isoforms are considered, it seems that the three enzymes of importance are AKR1C1, AKR1C2, and AKR1C4. AKR1C1 and AKR1C2 predominantly catalyze the formation of 3β-hydroxytibolone and are expressed in peripheral target tissues as well as in the liver. However, AKR1C4 is exclusively expressed in the liver and predominantly catalyzes the formation of 3α-hydroxytibolone. Therefore, these data may account for the fact that 3β-hydroxytibolone is the major metabolite in tibolone target tissues and 3α-hydroxytibolone is the major metabolite in the circulation (Blom, 2001; Timmer et al., 2002; Vos et al., 2002).

A unique phenomenon for AKR1C-catalyzed reactions was observed in the steady-state kinetic parameters for tibolone reduction by AKR1C2 (Fig. 4). A significant apparent substrate inhibition occurred at low tibolone concentrations. The best fit to the data were obtained using an equation for substrate inhibition in the nonlinear curve-fitting analyses (see *Materials and Methods)*, which yielded a submicromolar K_{iapp} value for the presumed inhibitory SES complex (Table 1).

In the presence of NAD^+, 3-hydroxytibolone was efficiently oxidized by homogeneous recombinant AKR1C2 and AKR1C4 (Figs. 5 and 6; Table 2), whereas homogeneous recombinant AKR1C1 and AKR1C3 merely acted as very poor 3-hydroxytibolone oxidases. The results revealed several remarkable aspects: 1) AKR1C1 acted as a poor 3-hydroxysteroid oxidase on either diastereomer similar to the previous results obtained with 3α- and 3β-androstanediol (Steckelbroeck et al., 2004); 2) AKR1C2 inverted its stereospecificity from an efficient 3α-hydroxysteroid oxidase with 3α-androstanediol as substrate to an efficient 3β-hydroxysteroid oxidase with 3β-hydroxytibolone, similar to the reductive direction; 3) whereas AKR1C3 acted as an efficient 17β-hydroxysteroid oxidase on 3α-androstanediol (Penning et al., 2000; Steckelbroeck et al., 2004), it did not catalyze the oxidation of the 17β-hydroxy moiety of 3α/β-hydroxy(tibolone), because the synthetic steroids contain an ethinyl group in the 17α-position (Scheme 1); 4) whereas AKR1C4 exclusively acted as an efficient 3α-hydroxysteroid oxidase on 3α-androstanediol (Steckelbroeck et al., 2004), it catalyzed the oxidation of both 3α- and 3β-hydroxytibolone with 3α-HSD activity being the more significant activity; and 5) similar to the previous results with 3α-androstanediol (Steckelbroeck et al., 2004), AKR1C4 acted as an in vitro epimerase in the oxidative direction with both diastereomers. In the first step of this epimerase reaction the hydroxysteroids are oxidized to yield tibolone and NADH, and in the second step tibolone is reduced by transferring the hydride from NADH to the other face of the steroid molecule. This epimerase reaction is similar to the one described for dTDP-glucose 4,6-dehydratase and is equivalent to the one described for RoDH-like 3α-HSD (Chetyrkin et al., 2001; Gerratana et al., 2001).

Previous studies using 5α-DHT and 3α-androstanediol demonstrated that, in transfected COS-1 and PC-3 cell lines, AKR1C2 worked exclusively as a 3-ketosteroid reductase (Rižner et al., 2003). Moreover, we have shown that, in vitro, the NAD^+-dependent oxidation of 3α- and 3β-androstanediol by the AKR1C isoforms was potently inhibited by low micromolar NADPH concentrations, whereas NADPH-dependent 3-ketosteroid reduction of 5α-DHT was not inhibited by the opposing cofactor NAD^+ (Steckelbroeck et al., 2004). Identical results were observed for the NAD^+-dependent oxidation of 3α- and 3β-hydroxytibolone and the NADPH-dependent reduction of tibolone, respectively (Fig. 7). Therefore, the in vivo direction of tibolone metabolism by the AKR1C enzymes will be dictated by the ratio of reductive and oxidative cofactors. In cells, the major reducing cofactor is NADPH and the

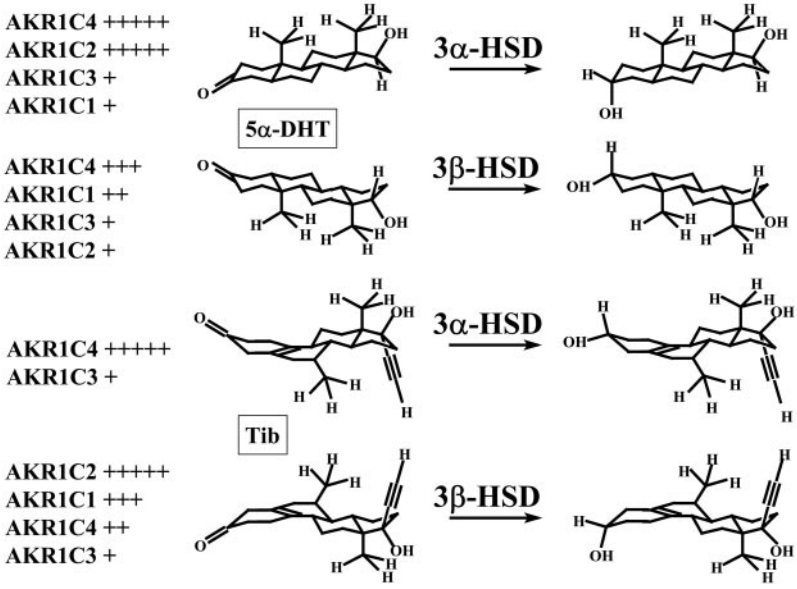

Scheme 2. Binding modes of tibolone (Tib) and 5α-DHT to achieve 3-ketosteroid reduction via 3α- or 3β-HSD activity of the AKR1C isoforms. For 3α-HSD activity, the β-face of the steroid molecule has to be directed toward the 4-*pro*-R hydrogen of the cofactor for hydride transfer, whereas for 3β-HSD activity, the α-face of the steroid molecule has to be directed toward the 4-*pro*-R hydrogen. The 4-*pro*-R hydrogen would be positioned above the plane of the steroid molecules pointing toward the C3-ketone group. Relative activities of the human AKR1C isoforms are given at the left margin of the scheme.

major oxidative cofactor is NAD^+: in the cytosol the [NADPH]/[$NADP^+$] ratio approaches 100:1 and the [NADH]/[NAD^+] ratios approaches 1:1000 (Krebs, 1973; Reich and Sel'kov, 1981). This strongly suggests that all AKR1C isoforms will reduce tibolone in vivo, but it is unlikely that the enzymes will oxidize 3α- and 3β-hydroxytibolone in vivo.

Previous molecular docking simulations using crystal structures of AKR1C1 and AKR1C2 rationalized why AKR1C1 predominantly acts as a 3β-HSD toward 5α-DHT, whereas AKR1C2 acts as a 3α-HSD toward 5α-DHT (Steckelbroeck et al., 2004). To explain why AKR1C2 inverted its stereospecificity from a 3α-HSD with 5α-DHT to a 3β-HSD with tibolone, whereas AKR1C1 retained its stereospecificity as a 3β-HSD with 5α-DHT and tibolone, we report molecular docking simulations of tibolone binding to the active sites of the two AKR1C isoforms. These simulations indicated that tibolone is bound in a similar manner in the active sites of both isozymes, in which the synthetic 19-nor-3-ketosteroid (possessing a long α-oriented ethinyl group at C17) was flipped upside down relative to the orientation of 5α-DHT in the binding pockets of the two proteins (Fig. 8; Scheme 2; see the positions of the C18 methyl groups in 5α-DHT and tibolone). The positions of tibolone in both isoforms depict the positional arrangement between tibolone and the cofactor for the formation of 3β-hydroxytibolone with the α-face of the steroid directed to the 4-*pro*-R hydrogen of nicotinamide for hydride transfer (Fig. 8A). In contrast, the preferred position of 5α-DHT docked into AKR1C2 was oriented for the 3α-HSD reaction with the A-ring of the steroid presenting its β-face to the 4-*pro*-R hydrogen (Fig. 8C), whereas the preferred position of 5α-DHT docked into AKR1C1 was oriented for the 3β-HSD reaction with the A-ring presenting its α-face to the 4-*pro*-R hydrogen of the cofactor (Fig. 8B). It is interesting that a high number of docking conformations describing nonproductive binding modes of tibolone in the active site of AKR1C2 were observed. These conformations with the C3-ketone group of the steroid distant from the cofactor had similar docking energies to the conformations describing the productive binding mode of tibolone. The high frequency of these nonproductive binding modes of tibolone in AKR1C2 (found 252 times of 256 runs) may account for the observed strong substrate inhibition.

In conclusion, our results demonstrate that cytosolic AKR1C1 and AKR1C2 work as efficient 3β-HSDs to catalyze the formation of 3β-hydroxytibolone, whereas cytosolic AKR1C4 acts predominantly as an efficient cytosolic 3α-HSD to catalyze the formation of 3α-hydroxytibolone. Considering the tissue-specific expression patterns of the human AKR1C isoforms, the profile of tibolone reduction catalyzed by these enzymes may explain the differences in the metabolic profile of tibolone in peripheral target tissues and the circulation. The profile of tibolone reduction catalyzed by the human AKR1C isozymes also suggests that the enzymes may be involved in the metabolism of contraceptive $\Delta^{5(10)}$-19-nor-3-ketosteroids (e.g., norethynodrel). These drugs are known to be reduced to their 3α- and 3β-hydroxymetabolites in the liver, endometrium, and myometrium, and the enzyme(s) responsible were found to be located in the cytosolic subcellular fraction (Palmer et al., 1969; Freudenthal et al., 1970; Martin et al., 1970; Murugesan et al., 1973).

References

Albertazzi P, di Micco R, and Zanardi E (1998) Tibolone: a review. *Maturitas* **30:**295–305.

Blok LJ, De Ruiter PE, Kuhne EC, Hanekamp EE, Grootegoed JA, Smid-Koopman E, Gielen SC, De Gooyer ME, Kloosterboer HJ, and Burger CW (2003) Progestogenic effects of tibolone on human endometrial cancer cells. *J Clin Endocrinol Metab* **88:**2327–2334.

Blom MJ (2001) Steroids and steroid analogues for hormone replacement therapy: metabolism in target tissues. Ph.D. dissertation, University of Utrecht, Utrecht, The Netherlands.

Bradford MM (1976) A rapid and sensitive method for the quantitation of microgram quantities of protein utilizing the principle of protein-dye binding. *Anal Biochem* **72:**248–254.

Burczynski ME, Harvey RG, and Penning TM (1998) Expression and characterization of four recombinant human dihydrodiol dehydrogenase isoforms: oxidation of *trans*-7,8-dihydroxy-7,8-dihydrobenzo[*a*]pyrene to the activated *o*-quinone metabolite benzo[*a*]pyrene-7,8-dione. *Biochemistry* **37:**6781–6790.

Chetrite GS, Kloosterboer HJ, Philippe JC, and Pasqualini JR (1999) Effects of Org OD14 (Livial) and its metabolites on 17β-hydroxysteroid dehydrogenase activity in hormone dependent MCF-7 and T-47D breast cancer cells. *Anticancer Res* **19:**261–267.

Chetyrkin SV, Hu J, Gough WH, Dumaual N, and Kedishvili NY (2001) Further characterization of human microsomal 3α-hydroxysteroid dehydrogenase. *Arch Biochem Biophys* **386:**1–10.

Colacurci N, Mele D, De Franciscis P, Costa V, Fortunato N, and De Seta L (1998) Effects of tibolone on the breast. *Eur J Obstet Gynecol Reprod Biol* **80:**235–238.

Couture J-F, Legrand P, Cantin L, Luu-The V, Labrie F, and Breton R (2003) Human 20α-hydroxysteroid dehydrogenase: crystallographic and site-directed mutagenesis studies lead to the identification of an alternative binding site for C21-steroids. *J Mol Biol* **331:**593–604.

Freudenthal RI, Cook CE, Twine M, Rosenfeld R, and Wall ME (1970) Metabolism of norethynodrel by rat liver. *Biochem Pharmacol* **20:**1507–1512.

Gerratana B, Cleland WW, and Frey PA (2001) Mechanistic roles of Thr 143, Tyr160 and Lys164 in the reaction catalysed by dTDP-glucose 4,6-dehydratase. *Biochemistry* **40:**9187–9195.

Gompel A, Chaouat M, Jacob D, Perrot JY, Kloosterboer HJ, and Rostene W (2002) *In vitro* studies of tibolone in breast cells. *Fertil Steril* **78:**351–359.

de Gooyer ME, Deckers GH, Schoonen WGEJ, Verheul HAM, and Kloosterboer HJ (2003) Receptor profiling and endocrine interactions of tibolone. *Steroids* **68:**21–30.

de Gooyer ME, Kleyn GT, Smits KC, Ederveen AG, Verheul HA, and Kloosterboer HJ (2001) Tibolone: a compound with tissue specific inhibitory effects on sulfatase. *Mol Cell Endocrinol* **183:**55–62.

Jin Y, Stayrook SE, Albert RH, Palackal NT, Penning TM, and Lewis M (2001) Crystal structure of human type III 3α-hydroxysteroid dehydrogenase/bile acid binding protein complexed with NADP+ and ursodeoxycholate. *Biochemistry* **40:**10161–10168.

Kloosterboer HJ (2001) Tibolone: a steroid with a tissue-specific mode of action. *J Steroid Biochem Mol Biol* **76:**231–238.

Kloosterboer HJ and Ederveen AGH (2003) Pros and cons of existing treatment modalities in osteoporosis: a comparison between tibolone, SERMS and estrogen (+/− progestogen) treatments. *J Steroid Biochem Mol Biol* **83:**157–165.

Krebs HA (1973) Pyridine nucleotides and rate control. *Symp Soc Exp Biol* **27:**299–318.

Lowry OH and Passonneau JV (1972) Flexible System of Enzymatic Analysis, New York: Academic Press.

Martin AP, Halterman DR, Vorbeck ML, Kuo MC, and Lucas FV (1970) Metabolism of norethynodrel, a 19-nor progestin: subcellular localization of enzyme activity. *Steroids* **16:**487–493.

Moore RA (1999) Livial: a review of clinical studies. *Br J Obstet Gynaecol* **106 (Suppl) 19:**1–21.

Morris GM, Goodsell DS, Halliday RS, Huey R, Hart WE, Belew RK, and Olson AJ (1998) Automated docking using a Lamarckian genetic algorithm and empirical binding free energy function. *J Comput Chem* **19:**1639–1662.

Murugesan K, Hingorani V, and Laumas KR (1973) *In vitro* metabolism of [6,7-^{3}H]norethynodrel in the human endometrium and the myometrium. *Acta Endocrinol (Copenh)* **74:**576–591.

Palmer KH, Ross FT, Rhodes LS, Baggett B, and Wall ME (1969) Metabolism of antifertility steroids. I. Norethynodrel. *J Pharmacol Exp Ther* **167:**207–216.

Pasqualini JR and Chetrite GS (1999) Estrone sulfatase versus estrone sulfotransferase in human breast cancer: potential clinical applications. *J Steroid Biochem Mol Biol* **59:**287–292.

Penning TM (1997) Molecular endocrinology of hydroxysteroid dehydrogenases. *Endocr Rev* **18:**281–305.

Penning TM and Talalay P (1983) Inhibition of a major NAD(P)$^+$-linked oxidoreductase from rat liver cytosol by steroidal and nonsteroidal anti-inflammatory agents and by prostaglandins. *Proc Natl Acad Sci USA* **80:**4504–4508.

Penning TM, Burczynski ME, Jez JM, Hung CF, Lin HK, Ma H, Moore M, Palackal N, and Ratnam K (2000) Human 3α-hydroxysteroid dehydrogenase isoforms (AKR1C1-AKR1C4) of the aldo-keto reductase superfamily: functional plasticity and tissue distribution reveals roles in the inactivation and formation of male and female sex hormones. *Biochem J* **351:**67–77.

Purohit A, Malini B, Hooymans C, and Newman SP (2001) Inhibition of oestrone sulphatase activity by tibolone and its metabolites. *Horm Metab Res* **34:**1–6.

Ratnam K, Ma H, and Penning TM (1999) The arginine 276 anchor for NADP(H) dictates fluorescence kinetic transients in 3α-hydroxysteroid dehydrogenase, a representative aldo-keto reductase. *Biochemistry* **38:**7856–7864.

Reich JG and Sel'kov EE (1981) *Energy Metabolism of the Cell: a Theoretical Treatise*. Academic Press, New York.

Rižner T, Lin HK, Peehl DM, Steckelbroeck S, Bauman DR, and Penning TM (2003) Human type 3 3α-hydroxysteroid dehydrogenase (aldo-keto reductase 1C2) and androgen metabolism in prostate cells. *Endocrinology* **144:**2922–2932.

Smith CL and O'Malley BW (2004) Coregulator Function: a key to understanding tissue specificity of selective receptor modulators. *Endocrine Rev* **25:**45–71.
Steckelbroeck S, Jin Y, Gopishetty S, Oyesanmi B, and Penning TM (2004) Human cytosolic 3α-hydroxysteroid dehydrogenases of the aldo-keto reductase superfamily display significant 3β-hydroxysteroid dehydrogenase activity: implications for steroid hormone metabolism and action. *J Biol Chem* **279:**10784–10795.
Timmer CJ, Verheul HAM, and Doorstam DP (2002) Pharmacokinetics of tibolone in early and late postmenopausal women. *J Clin Pharmacol* **54:**101–106.
Valdivia I and Ortega D (2000) Mammographic density in postmenopausal women treated with tibolone, estriol or conventional hormone replacement therapy. *Clin Drug Investig* **20:**101–107.
van de Ven J, Donker GH, Sprong M, Blankenstein MA, and Thijssen JH (2002) Effect of tibolone (Org OD14) and its metabolites on aromatase and estrone sulfatase activity in human breast adipose stromal cells and in MCF-7 and T47D breast cancer cells. *J Steroid Biochem Mol Biol* **81:**237–247.
Volker W, Coelingh Bennink HJ, and Helmond FA (2001) Effects of tibolone on the endometrium. *Climacteric* **4:**203–208.
Vos RME, Krebbers SFM, Verhoeven CHJ, and Delbressine LPC (2002) The *in vivo* human metabolism of tibolone. *Drug Metab Dispos* **30:**106–112.

Address correspondence to: Dr. Trevor M. Penning, Department of Pharmacology, University of Pennsylvania School of Medicine, 130C John Morgan Bldg., 3620 Hamilton Walk, Philadelphia, PA 19104-6084. E-mail: penning@pharm.med.upenn.edu